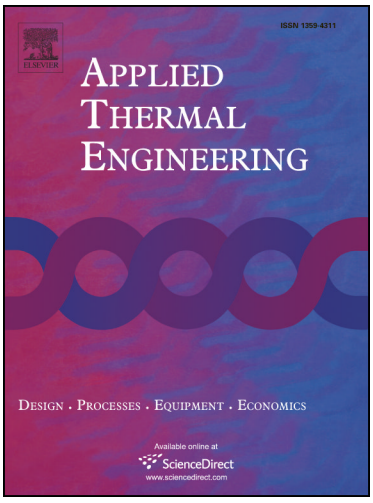

Research Paper

Self –Propelled Nanofluids a Path to a highly Effective Coolant

Yousef M.F. El Hasadi, Martin Crapper

PII: S1359-4311(17)30571-9
DOI: http://dx.doi.org/10.1016/j.applthermaleng.2017.08.050
Reference: ATE 10932

To appear in: *Applied Thermal Engineering*

Received Date: 25 January 2017
Revised Date: 17 July 2017
Accepted Date: 9 August 2017

Please cite this article as: Y.M.F. El Hasadi, M. Crapper, Self –Propelled Nanofluids a Path to a highly Effective Coolant, *Applied Thermal Engineering* (2017), doi: http://dx.doi.org/10.1016/j.applthermaleng.2017.08.050

Self –Propelled Nanofluids a Path to a highly Effective Coolant

by

Yousef M. F. El Hasadi[1] and Martin Crapper[2]

1-International Centre for Numerical Methods in Engineering (CIMNE), Edificio C1, Campus Norte, Jordi Girona 1-3,08034, Barcelona, Spain,

2-Department of Mechanical and Construction Engineering, Northumbria University, Ellison Place Newcastle upon Tyne, NE1 8ST, UK

Email:Yme0001@Auburn.edu

Abstract

We propose a new self-propelled nanofluid having advantageous thermal and rheological properties at the same time. The nanofluid consists of a low volume fraction of self-propelled particles known as Artificial Bacterial Flagella (ABF), which will swim as pushers in a manner similar to the swimming of E-coil microorganisms with flagella. A theoretical model is introduced, describing the mechanisms responsible for the reduction of viscosity. The model shows that the swimming velocity of the particle and its geometry play an essential role in the reduction of the suspension viscosity. The results obtained from the theoretical model compare qualitatively with experiments in the literature. The model shows a significant decrease in viscosity at very low volume fractions, and that the viscosity of the suspension is reduced as the volume fraction of the particles increases. Using an in-house finite volume code, we numerically simulate natural convection effects in our ABF self-propelled nanofuid inside a square cavity heated from its vertical sides. Simulations are conducted at volume fractions of 0.7%, 0.8% and 0.83%, comparing the performance of a self-propelled nanofluid with conventional non-active nanofluids (i.e. carbon nanotubes in water). The results show that the heat transfer rate measured by the Nusselt number is three times higher than for the case of classical nanofluids and pure water at the same operating conditions and 0.83% volume fraction of particles. Also, due to the very dilute volume fractions of particles in the proposed nanofluid, their stability can endure for long operating times. There is also a significant decrease in the viscosity (around 25 times lower than water) which will result in a significant reduction in the pumping power.

Keywords: Nanofluid; Self-Propelled particles; Heat transfer; viscosity; Simulation; Heat transfer Enhancement ; Artificial Bacterial Flagella.

Nomenclature

c_p	Specific heat (J/kgK)
$\vec{e}_y$	Unit vector in the *y*-direction
H	Length of the cavity (m)
k	Thermal conductivity (W/mK)
Ra	$\frac{\rho\beta(T_H - T_C)H^3}{\mu\alpha}$
p	Pressure (Pa)
t	Time (s)
T	Temperature (K)
$\vec{U}$	Velocity vector (m/s)
x, y	Cartesian coordinates (m)

Greek Symbols

α	Thermal diffusivity (m^2/s)
β	Coefficient of thermal expansion (1/K)
ρ	Density (kg/m^3)
μ	Dynamic viscosity (Pa. s)
ϕ	Volume fraction of particles
ε	Geometrical aspect ratio of the particle

Subscripts

c	Cold

f	Base fluid
h	Hot
in	Initial conditions
p	Particle
ref	Reference state

1 Introduction

The use of heat transfer fluids in many industrial applications has increased dramatically in the last 100 years. Heat transfer fluids are found in many applications such as the food industry, heating and cooling of vehicles, aircraft, computing systems and space systems. Also, they are used to heat and cool residential buildings and in chemical processing industries such as oil and paper production. However, conventional heat transfer fluids such water suffer from low thermal conductivity which constrains their efficiency in transferring heat.

More than 20 years ago, Choi and Eastman [1] proposed an innovative way to enhance the thermal conductivity of heat transfer liquids by suspending passive metallic and non-metallic nano-size particles in the heat transfer fluids. They named the resulting colloidal suspensions "nanofluids". Their idea is based on the fact that suspending particles that are orders of magnitude more conductive than the host medium (i.e. liquid) will increase the overall thermal conductivity of the mixture as predicted by effective medium theory [2]. Nanofluids triggered an enormous amount of research by the international scientific community, and soon the first results of a significant increase of the overall thermal conductivity of nanofluids started to appear [3, 4] with overall thermal conductivity increased by 40% and 150 % respectively for low volume fractions of the particles. There are excellent reviews in the literature that deal with the thermal transport properties of nanofluids [5, 6, and 7]. It is found that clustering, layering at the solid/liquid interface and ballistic phonon transport are the main mechanisms responsible for the enhancement of the thermal conductivity of nanofluids [8].

However, for nanofluids to be used as heat transfer fluids, they must not only possess great thermal properties, but also suitable rheological properties. An over-increase in the viscosity of

the suspension will lead to the growth of the pumping power requirement, and also suppress natural convection [9, 10]. Studies started to report that the enormous increase in the viscosity of the nanofluids with the increase of the volume fraction of the particles [11, 12] resulted in a significant decrease of their efficiency as heat transfer fluids. A simple criterion proposed by [9] for assessing the efficiency of using nanofluids as heat transfer fluids states that the ratio between the enhancement of the viscosity to that of the thermal conductivity must not be more than 4.0.

Nanofluids are a class of non-active colloidal suspensions; non-active colloids are those that cannot self-propel. Their rheology has been understood for some time. Einstein [13] was the first to predict that the viscosity of a suspension increases linearly with the volume fraction of the particles due to the dissipation of energy resulted from the movement of the particles within the host solvent. Einstein's simple formula [13] assumed that the concentration of the particles is very dilute, usually less than 0.01 by volume. In those types of conditions the particles in the suspensions do not interact with each other hydrodynamically or by any other inter-particle force. It needed more than 60 years for the scientific community to prove the correctness of Einstein formula [14] experimentally, because it is difficult to achieve all the necessary conditions set by Einestein [13] in the laboratory. The first investigations related to nanofluids assumed that the nanofluid suspensions will follow [13]; however, the majority of the experimental investigations showed that the viscosity of the suspensions increased significantly more than linearly with an increasing volume of particles [10]. The deviation of the effective viscosity from the Einstein [13] prediction can be attributed to several factors; among them are the hydrodynamic interactions between the particles, inter-particles forces such as Van der Waals, steric forces resulting from coating the particle surfaces with polymers such as surfactants, electrostatic forces resulting from the ionic clouds around the surface of the particles, particle clustering, shear rate, and finally particle shape. An excellent reference that elaborates the mechanisms involved in the rheology of colloidal suspensions is given by [15]. Nanofluids containing spherical particles exhibit more of a Newtonian behaviour at low volume fractions, while nanofluids containing non-spherical particles such as rods show non-Newtonian behaviour at the same low volume fractions. However, both nanofluid types shows non-Newtonian behaviour including shear thinning at high shearing rates [10]. Also, nanofluids show a decrease in viscosity as their temperature increased; however this behaviour is reversed when a certain

critical temperature is reached, and beyond this temperature the viscosity increases again [16]. In general, for conventional nanofluids, there be always an increase in viscosity as the volume fraction of the particles increases, and thus their efficiency as heat transfer fluids will deteriorate.

In this paper, we will try to answer the very simple question which is can we create a nanofluid in which the thermal conductivity will increase with the volume fraction of particles, while its viscosity will decrease, thus creating a predominate efficient coolant?

A research field that can shed light on this question is that of the active matter, a close relative to the colloidal suspension field. Active matter is an emerging new area of research, which includes under its umbrella various types of systems such as colloidal particles and microorganisms that convert some form of energy (typically chemical) into mechanical work. Examples of such systems include motile bacteria, microscopic algae, solutions of motor proteins, human sperm, reactive driven colloidal suspensions, self-propelled nanotubes and shaken granular materials [17]. The generation of mechanical work by active matter results in a change in their microstructure, either by direct contact or by long range and complex hydrodynamic interactions. The manifestations of these interactions include spontaneous unsteady flows at mesoscopic length scales, the formation of complex patterns and the generation of direct collective motion [17].

The two most distinct ways that rod-type self-propelled particles and living organisms swim are the pusher and the puller. The propulsion of pushers such E-coli bacteria is achieved by rotating a flagella bundle pushing the fluid behind the bacterial body, while the puller typically propels itself by conducting a breaststroke-like motion with multiple flagella attached to their body. The great example of pullers is that of algae. The rheology of suspensions containing particles that swim as pullers is similar to that of non-active colloidal suspensions, in which the suspension viscosity increases with the volume fraction of the particles [17].

Recently, the rheological properties of active matter have demonstrated a fascinating behaviour in which the viscosity of a suspension of bacteria which swim as pushers was less than that of the solvent. This is in clear contradiction with the known results of non-active (i.e. passive) suspension rheology. Sokolov and Aranson [18] measured the viscosity of an active suspension consisting of Bacillus Subtilis, a rod shape bacterium (pushers) about 5 microns long and 0.7

microns in diameter. The bacteria were grown in Terrific Broth medium. The swimming velocity of the bacteria (i.e. motility) can be controlled by the amount of the oxygen dissolved in the solvent: the lesser the amount of oxygen, the slower the bacteria move. It was found that the viscosity of the suspension with the motile bacteria is about seven times lower than that of the solvent. The reduction was found to be a function of the bacteria swimming velocity and the concentration of the bacteria. The researchers observed that the viscosity of a suspension with dead bacteria is higher than that of the solvent. Gachelin et al. [19] showed similar results to those of [18] for E. coli bacteria (pushers). Lopez et al. [20] showed experimentally that for a low volume fraction of hyper active E. coli bacteria (pushers), the state of super fluidity is reached. Superfluids are a special state of the liquid where the viscosity is zero.

There are very few investigations that deal theoretically with the rheological behaviour of active colloidal suspensions. Haines et al. [21] investigated the behaviour of dilute active colloidal suspensions (i.e. no hydrodynamic interaction between the particles); they demonstrated that a rotational nose (rotational difussivity) must exist for the reduction of the viscosity to be achieved for self-propelled colloidal particles (pushers) that have a rod shape. Rayan et al. [22] investigated numerically and analytically the behaviour of self- propelled particles. They found that a reduction of the viscosity of the suspension can be achieved also, by the hydrodynamic interactions between the particles. All the previous theoretical investigations of active matter are based on numerical simulations of rods swimming as pushers, and show a similar behaviour of viscosity reduction to experiments conducted for bacterial suspensions. However, what is missing is a simple relation that shows the main physical ingredients involved in the rheology of the active matter. Recently Matilla et al. [23] investigated numerically and analytically the rheology of active rod-shaped particles at a microfluidic length scale. They developed a simple theory that describes the anomalous rheological behaviour of the self-propelled particles. They stated that the swimming rod particle is exerting active stress on the fluid and the particles are naturally buoyant, and thus the disturbance that they impose in surrounding flow is dipole in nature. This disturbance can hinder the flow depending on the sign of the dipole (known as the activity). For the case when the sign of the dipole is positive (pullers) they observed that their rheological behaviour is similar to the non-active colloidal suspensions, in which the viscosity increases with the volume fraction of the particles. On the other hand, if the sign of the dipole is negative, they observed that the viscosity of the suspension is decreased, and even negative

viscosity is reported. Using kinetic theory, the authors came up with an analytical formula for the relative viscosity of active suspensions at the dilute limit. The proposed formula shows that the relative viscosity is a function of the volume fraction of the particles, the strength and sign of the dipole, swimming velocity of the particles and the geometrical features of the particles.

In the coming sections, the proposed formula by [23] will be introduced and discussed. Also, the authors [23] numerically verified the experimental observations of [20], where a super-fluid state is reached by using pusher swimming particles.

Substantial research related to self-propelled particle suspensions is related to controlling the movement and the orientation of the particles in different concentrations. Katuri [24] discussed self-propelled particles that had been developed to move a long prescribed concentration gradients, or swim against gravity. Very recently, the first self-propelled nanofluid has been developed by Luo et al. [25], composed of graphene-based Janus amphiphilic nano-sheets in a saline environment. They found that the nanosheets spontaneously approach an oil-water interface, reducing significantly the surface tension, and thus increasing the availability of the oil in the recovery process.

In the current paper, we propose a new type of a nanofluid based on ABF particles, taking into account new advancements in the field of the active colloidal suspensions. The nanofluid we propose will consist of self-propelled ABF particles which swim as pushers, suspended in water and propelled in a similar way to bacteria with flagella. Adding the self-propelled particles will create a mechanism that will allow for an increase in thermal conductivity combined with a decrease in viscosity with increasing volume fraction. This is the first time such a nanofluid has been proposed, and its ability to serve as heat transfer fluid will be tested. A theoretical model for the viscosity of the active colloidal suspensions will be introduced, and the viscosity reduction will be explained. In the second part of the paper, the nanofluid will numerically tested for the case of natural convection inside a square cavity heated from a vertical side.

2 Self-Propelled Artificial Bacterial Flagella (ABF) Particles

We propose two types of self-propelled particles: one that is based on a metallic micro- or nano-metallic rods, and another based on carbon nanotubes. Both types of particles are highly conductive, and they are both types of ABF. The universal accepted definition of the nanofluids

is that they are colloidal suspensions of highly conductive particles, and the accepted range of colloidal particles size is between 1nm to 1μm [26]. If the particle size exceeds that the of 1μm the suspensions either called non-colloidal in this regime the effects of the Brownian motion can be neglected or called granular material where the inertia of the particle plays an essential role in their motion [27]. In the micrometer size range, the proposed nanofluids are in the non-colloidal regime; it is shown in the literature that Brownian motion does not play a significant role in the enhancement of the thermal properties of the nanofluid. Also, the name nanofluid is attached with suspensions that exhibit improvement in their thermal conductivity, and this is why we want to keep it. Metallic micro-rod particles that mimic the motion of E-coli bacteria have been manufactured by Zhang et al. [28]. These consisted of two parts, a head and a tail. The nanobelt tail resembled the natural shape and length of a flagellum, and the metallic magnetic head was in the shape of a thin square plate. The physical dimensions of the tail were 1.8μm in diameter and 38 μm in length, while the head had a thickness of 200nm and a length of 2.5 μm. The ABFs were designed for a controlled swimming motion in low Reynolds number regimes. They can change direction by just changing the rotation direction of their tail by alternating the magnetic field. The manufacturing method that the authors in [28] used can produce around 3 million ABF particles at once. They were tested in water, as a single particle and in multiple particle formations. They achieved swimming speeds of the order of 18 $\mu m.s^{-1}$. One of the great benefits of using the ABF type of particles is that we can achieve a controlled motion of swarms of particles, as opposed to bacteria that need a substantial time to find their direction due to tumbling. Also, with ABF particles, clustering can be avoided.

Ghosh and Fischers [29] developed a new method to produce smaller ABF particles and in large numbers. Their method is the glancing angle deposition; they managed to produce 10^9 ABF particles of SiO_2 per cm^2. The diameter of the particles was 200-300 nm and their length was 1-2 μm, and they achieved swimming speeds in water of an order of 25 $\mu m.s^{-1}$. Very recently Huang et al. [30] developed ABF particles where the particle shape can be reconfigured.

We have selected carbon nanotube geometry as a second choice for several reasons beyond its extraordinary thermo-physical properties. Carbon nanotubes have very similar geometry to that of the natural flagella responsible for propelling the E-coli bacteria; they are strong, and also they can bend - an essential property to mimic the swimming behaviour of the flagella. Carbon

nanotubes have been proposed to be used as flagella to move micro-robots to break kidney stones inside the human body [31], where the nanotubes were to be propelled by a magnetic field. Foroughi et al. [32] reported the first case of an ABF carbon nanotube swimming in an electrolyte solution. The propulsion of the carbon nanotube ABF was achieved by controlling the electric double layer thickness around the ABF surface. Carbon nanotubes can be propelled by using different types of energy such chemical and heat [33]. Recently [34] reported the production of helical shape carbon nanotubes, that had a lot of similarities with the ABF in [32], with different quantities and sizes.

The preceding paragraph shows the feasibility of the production of ABF micro-nano particles that can mimic the motion of E-coli bacteria, which is the main reason behind the significant reduction of the reported viscosity [20]. Also, it shows that we could produce those particles from different conductive materials, plus controlling their motion, velocity and orientation. The proposed shape of the self- propelled ABF particles is shown in Figure 1, which is a similar shape to the one reported in [28].

3 Viscosity Model and Heat Transfer Efficiency of Self-Propelled Nanofluids

Here we present a viscosity model that explains the richness of the rheological behaviour of active colloidal suspensions, and the brief overview of the efficacy of using self-propelled nanofluids. Self-propelled nanofluid is reducing the viscosity of the host fluid because the particles create a stretching pathway in the extensional shearing direction [23]. This stretching pathway makes the fluid moving easier and faster, and thus reducing the overall viscosity. The stretching of the fluid is reflected in Eq. (1) by the negative sign of the activity stress.

The constitutive law that governs the relationship between the ratio of the viscosity of the suspension of rod active particles and that of the solvent is derived in [23] and is given by the following relation:

$$\mu_{\mathrm{r}} = 1.0 + (\frac{1}{30})(\alpha\zeta + 2\beta) \tag{1}$$

where α, and β are given from the following relations:

$$\alpha = \frac{n}{\mu_{\mathrm{f}} D_{\mathrm{r}}} (\pm \sigma_0) \tag{2}$$

$$\beta = \phi A \ . \tag{3}$$

Here, n, μ_{f}, D_{r}, σ_0, ζ and ϕ are the number density of the particles, the viscosity of the solvent, the rotational diffusivity of the particles, the activity of the particles, the Bretherton constant, and finally the volume fraction of the particles. A is given by the following relation:

$$A = \frac{\pi}{6 Log_{10}(2\epsilon\ )} \tag{4}$$

where ϵ is the aspect ratio of the rod particle $(\frac{l}{a})$, l and a being the length and the diameter of the particle.

As demonstrated from Eq. (1), the viscosity of the active colloidal suspension is a result of the summation of two stresses, one that results from the activity of the particles (αζ), and one that results from the presence of the particles in the liquid (2β). The sign of the stress that results from the activity of the particles alternates with the way that the particles swim. For the case of pullers, σ_0 is positive, whereas for the case of the pushers it is negative. Eq. (1) Helps to elucidate the dramatic reduction of the viscosity observed in [20]. To mathematically close the model, the rotational diffusivity of the self-propelled particles is given as the following [35]:

$$D_r = \frac{3k_{\mathrm{b}}T}{\pi \mu_{\mathrm{f}} l^3} (Log_{10}(\tfrac{\epsilon}{2}) - 0.66) \ . \tag{5}$$

k_b and T are the Boltzmann constant and the absolute temperature of the suspension respectively. Finally, the activity of the rod self-propelled particles is given from the following relation [36]:

$$\sigma_0 = \pm\left(\frac{213\pi}{14}\right)\mu_{\mathrm{f}} l^2 \bar{v} \ . \tag{6}$$

Here $\bar{v}$ represents the average swimming velocity of the self-propelled particles.

3.1 Implementation of the Viscosity Model for Self-Propelled Particle Suspensions

The suspensions considered consist of ABF particles suspended in water, and are made of carbon nanotubes. Carbon nanotubes are chosen because there is a significant amount of literature about their thermo-physical properties. However, the material of the particles could be metallic, or non-metallic in nature. Eq. 1 shows that the active stress that self-propelled particles impose on the fluid depends on the rotational diffusivity of the rod particles and their activity. The variation of these properties with the aspect ratio and length of the particles is thus essential for understanding the viscosity reduction mechanism. The rotational diffusivity increases as the aspect ratio of the particles increases and increases significantly as the length of the particles decreases, as shown in Figure 2. For example, the difference between the values of the rotational diffusivity between particles that are $1x10^{-7}$m, and $1x10^{-5}$m in length is about four orders of magnitude. This implies that the mechanism of viscosity reduction will be less efficient if the particles are in the nano size range, since the active stress is inversely proportional to the rotational diffusivity. The activity of the particles increases with the length of the particles, and is strongly dependent on the velocity of the particles as shown in Figure 3.

To test the predication capabilities of Eq. 1, a comparison is made with the experimental results of [20] in the dilute regime, where the hydrodynamic interactions are weak. The authors of [20] proposed the following equation resulting from curve fitting of their experimental results:

$$\mu_{\mathrm{r}} = (1.0 - 120\phi) \ . \tag{7}$$

The parameters that were used as inputs in our comparison were the length of the E-coli bacteria (l = 2 μm), the swimming velocity of bacteria ($\overline{v_0}$ = 28 $\mu m s^{-1}$), and the volume fraction of the bacteria, as reported in [20]. The comparison is shown in Figure 4. Eq. 1 captures qualitatively the linear decrease in the relative viscosity, which is an essential feature of the rheology of active matter. Also, Figure 3 demonstrates that self-propelled nanofluids can achieve a significant reduction in the viscosity of the suspension at very low volume fractions. For example, at ϕ = 0.0025, the theory (Eq.1) predicts a reduction of about 20%, while experiments [20] show a decline of about 30%.

The discrepancy between the theoretical and the experimental results may be due to several factors, such the accuracy of the size and swimming velocity of the bacteria measurements and the involvement of other phenomena such as the hydrodynamic interactions. However, even with the difference between the theory and experiments, Eq. 1 can be a good starting point for the prediction of the rheology of the self-propelled nanofluids.

The effect of the variation of the swimming velocity of the particle is shown in Figure 5. For a very low swimming velocity ($\overline{v_0}$ = 1.0 $\mu m s^{-1}$), there is not a significant reduction in the relative viscosity. However, as the swimming velocity increases to $\overline{v_0}$ = 28 $\mu m s^{-1}$, a significant reduction in the viscosity is achieved, for example for the case of ϕ = 0.03, the viscosity of the suspension is about 90% less than that of the solvent. This reduction is attributed to the increase in the activity of the particles, and thus an increase in the negative value of the activity stress.

Another geometrical parameter of the particle geometry is the aspect ratio. The variation of the relative viscosity of the suspension for different volume fractions, and aspect ratios are plotted in Figure 6. For investigating the effect of the aspect ratio, we selected the length of the particles to be l = 1.0 μm, and two values for the swimming velocities ($\overline{v_0}$ = 1 and 50 $\mu m s^{-1}$). As shown from the figure, there is an optimum value for the aspect ratio in which the maximum reduction in the viscosity occurs, regardless of the swimming velocity. In the current case it is ε = 10. The nonlinear behaviour can be explained because both the rotational diffusivity and the parameter A are both functions of the aspect ratio. A more in depth investigation is needed to elucidate the full effects of particle aspect ratio.

A very interesting result is shown in Figure 7, which illustrates the variation of the relative viscosity with the volume fraction for different lengths of particles. It shows that for of lengths near to the nanoscale, the suspension viscosity is equal to that of the solvent (i.e. water), and no viscosity reduction is observed. This is due to the dependence of the rotational diffusivity inversely with the cubic length of particles Eq. (5). Thus, making the rotational diffusivity to increases significantly as shown in Figure 2, and that contributes to the reduction of the active stress, and thus the reduction viscosity mechanism disappears. As the length of the particles increases to micro size, the relative viscosity is however reduced significantly due to the rotational diffusivity reduction and the increase of the activity stress.

3.2 Assessing the Effectiveness of the Self-Propelled Nanofluid:

A general purpose of developing nanofluids is to be used where convective heat transfer is essential. Prasher et al. [9] developed very simple criteria to assess the efficiency of nanofluids by developing an efficiency parameter, given by the following:

$$\Omega = \frac{\mu_{\mathrm{r}}}{k_{\mathrm{r}}} \tag{8}$$

where

$$k_r = \frac{k}{k_f} = \frac{k_{\mathrm{p}} + 2k_{\mathrm{f}} - 2\phi\left(k_f - k_{\mathrm{p}}\right)}{k_p + 2k_f + \left(k_f - k_{\mathrm{p}}\right)} \quad . \tag{9}$$

Where k_f, and k_p are the thermal conductivities of the solvent, and the particles respectively. Ω must be less than 4.0 for the nanofluid to be efficient. As shown from Figure 8, all the self-propelled nanofluids ($\overline{v_0}$ > 0) demonstrated are highly effective, since their efficiency parameter is always less than 1.0, and it decreases as the volume fraction increases. On the other hand, for the non-active colloids ($\overline{v_0}$ = 0.0 $\mu m s^{-1}$) the efficiency parameter is always greater than 1.0, and it increases with the volume fraction.

4. Modeling Self-propelled Nanofluids for case of Natural Convection

In this section, we test the capabilities of self-propelled nanofluids for the case of heating inside a square cavity, a case where the natural convection heat transfer mechanism will dominate. The self-propelled nanofluid is an ABF made from carbon nanotubes of size 1 micron suspended in water. we assume that the particles are moving with a velocity that can induce a particular change in the effective viscosity of the suspension, and we assume that the suspensions are extremely dilute, and uniformly distributed. We did not include anything about controlling the velocity and the orientation of the particles for the following two reasons. The first reason is that Eq. (1), in the manuscript shows that the effective viscosity is not a function of the orientation of the self-propelled particles, or the direction of their swimming, these assumptions are valid if the volume fraction of the particles is kept in the dilute limit. The second reason is that we did not decide yet about the most proper way to control the particles. We give emphasis to the magnetically controlled particles, but there are other paths such as temperature controlled self-propelled particles, light controlled self-propelled particles, and other ways of propelling particles.

We assumed a homogeneous mixture of ABF nanotubes and the solvent, that can be justified due to the very low volume fraction ($\phi < 5\%$) of the self-propelled particles used. The mathematical model is the classical mixture model in two dimensions, and consists only of the transport of momentum of fluid and heat, which are linked together via the buoyancy term, with the density changing according to the Boussinesq approximation. The effect of the nanotubes is only included in the effective transport properties. This specific model has been used extensively for simulating nanofluid behaviour [37, 38]. For the justification of using a single continuity for the fluid and the particles, we calculated the Schmidt number that represents the ratio between the momentum diffusion to the particle's diffusion ($Sc = \frac{\mu}{D_r \rho a^2}$), where a is the diameter of the particle. In more specifics, we calculated the Sc for the case the self-propelled nanofluids and non-active nano-fluids for the volume fraction of 0.8%, the Sc = 1.82 x10^6, and 7.12x10^4 for the non-active and active nanofluids respectively. The values of the Sc illustrate the significance of the momentum diffusion over the particle diffusion. Very recently [39] they show that the for

nanofluids with Sc> 1000 the mass transport does not play a significant role in the evolution of heat transfer and friction factor, for this reason, we did not use a separate transport equation for the particles. The fluid flow model that we used is based on the one-way coupling idea, in which the suspended particles do not play any significant role affecting the fluid flow around them. We use the nondimensional parameter defined in [27] $\Pi = \frac{\phi}{\frac{\rho_f}{\varrho_p}}$, which most have a value of less than 0.1, for the one-way coupling to be applied. For example, for the case of φ =0.8%, it equals to 0.01 which is sufficiently less than 0.1, and thus justify the usage of the one-way coupling in our simulations. The governing equations are the following:

Continuity:

$$\nabla \bullet \left(\rho \vec{U} \right) = 0 \tag{10}$$

Momentum:

$$\frac{\partial \rho \vec{U}}{\partial t} + \nabla \bullet \left(\rho \vec{U} \vec{U} \right) = -\nabla p + \mu \nabla^2 \vec{U} + \left(\rho \beta \right) g \left(T - T_{ref} \right) \vec{e}_y \tag{11}$$

Energy:

$$\rho c_p \frac{\partial T}{\partial t} + \nabla \bullet \left(\rho c_p \vec{U} T \right) = \nabla \bullet \left(k \nabla T \right) . \tag{12}$$

4.1 Initial and Boundary Conditions

The geometry of the physical problem tested is shown in Figure 9. The self-propelled nanofluid is contained in a square cavity (H = 10 mm) heated and cooled from the vertical sides, while the top and bottom sides are kept thermally isolated. The initial conditions are as follows:

$$\left\{\vec{U}_{in} = 0.0,\ T_{in} = 293K, \phi = (0.0083, 0.008, 0.007, 0.0\right\}.$$

(13)

For t > 0, the dimensional boundary conditions are as follows:

$$\left.\begin{array}{l} \vec{U} = 0, \dfrac{\partial T}{\partial y} = 0,\ for\ 0 \le x \le H,\ y = 0 \\ \vec{U} = 0, \dfrac{\partial T}{\partial y} = 0,\ for\ 0 \le x \le H,\ y = H \\ \vec{U} = 0, T = 303K,\ for\ 0 \le y \le H,\ x = 0 \\ \vec{U} = 0, T = 293K,\ for\ 0 \le y \le H,\ x = H \end{array}\right\}.$$

(14)

4.2 Mixture Relations and Effective Thermophysical Transport Properties

Self-propelled nanofluids can be considered as colloidal suspensions in the very dilute limit ($\phi < 5\%$) . Therefore, the well-known mixture relations will be used to evaluate their thermo-physical properties as a function of the volume fraction of the particles (ϕ). The density of the self-propelled nanofluids, their heat capacity and the compressibility coefficient used in the Boussinesq terms are therefore calculated as the follows:

$$\rho = (1-\phi)\rho_f + \phi\rho_p$$

(15a)

$$\rho c_p = (1-\phi)(\rho c_p)_f + \phi(\rho c_p)_p$$

(15b)

$$\rho\beta = (1-\phi)(\rho\beta)_f + \phi(\rho\beta)_p.$$

(15c)

The thermal conductivity of the suspension is calculated by the Maxwell relation, based on the effective medium theory as shown in Eq. (16):

$$k = k_{\mathrm{f}} \frac{k_{\mathrm{p}} + 2k_{\mathrm{f}} - 2\phi\left(k_f - k_{\mathrm{p}}\right)}{k_p + 2k_f + \left(k_f - k_{\mathrm{p}}\right)}$$

(16)

Since the field of active colloids is a new and emerging, for the current simulations the variation of viscosity will be calculated using the equation proposed by [40], utilizing experimentally based parameters. Following [40], for the variation of the viscosity of an active colloidal suspension of pushers:

$$\mu = \mu_{\mathrm{f}}\left(1 - \mathrm{K}\phi\right)$$

(17)

The constant *K* depends on several parameters such the swimming velocity of the particles, the inter-particle forces, the concentration of particles, the shear rate, and the shape of the particles. We obtained our value of *K* from the experimental work of [20]; according to their findings its value is 120 for a range of shear rates from 0.022 to 0.0755 s^{-1}, that are suitable for applications such as those considered in the current paper. Eq. 7 is a special case of Eq. 17, when *K* = 120.

The reason that we did not use Eq.1 is that we wanted to test the whole spectrum of the available relations in the literature, thus obtaining a better picture of the behaviour of self-propelled nanofluids. Also, as we saw previously in Figure 4, both Eq.1 and Eq.17 are qualitatively similar.

We also use non-active nanofluids for the sake of comparison with their self-propelled counterparts. Their thermal physical properties will be calculated using Equations (15a, 15b, 15c, and 16), while their effective viscosity is calculated form the following equation:

$$\mu = \frac{\mu_{\mathrm{f}}}{(1-\phi)^{2.5}} \tag{18}$$

Where μ, and μ_f are the viscosities of the suspension, and the solvent respectively. The non-dimensional parameter Rayleigh number governors the relation between the buoyancy and viscous forces, as the Rayleigh number increases the convection currents intensifies and the mixing process of the cold and hot streams of the fluid is more effective. The Rayleigh number is defined as the following:

$$\mathrm{Ra} = \frac{\mathrm{g}\beta(\mathrm{T_H} - \mathrm{T_C})\mathrm{H}^3}{\mu\alpha} \ . \tag{20}$$

Another non-dimensional parameter that is a mean indicator about the rate of the heat transfer is the Nusselt number (*Nu*). The value of the local *Nu* is calculated along the heated wall, from the following relation:

$$\mathrm{Nu} = \frac{\mathrm{qH}}{\mathrm{k}(\mathrm{T_H} - \mathrm{T_C})} \tag{21a}$$

and the average *Nu* along the hot wall is calculated from the following relation:

$$\overline{\mathrm{Nu}} = \frac{1}{\mathrm{H}} \int_0^{\mathrm{H}} \mathrm{Nu} \quad \mathrm{dy} \ . \tag{21b}$$

The thermo-physical properties of the pure water (solvent) and the carbon nanotubes are obtained from [41], [42] and are listed in Table 1.

Since the ABF particles were swimming by using a magnetic field to rotate their flagella, a suitable analysis is needed to see if the magnetic field had any effect on the flow field and

thus the Nusselt number. For the magmatic field to have a significant effect on the Nusselt number the magnetic force has to overcome that of the viscous force as experiments and numerical simulations show for the magnetic nanofluids [43,44]. The nondimensional Hartmann number that can be defined as the following:

$$Ha = B\,H\sqrt{\frac{\sigma}{\mu_f}}$$

B, and σ are the magnetic field and the electrical conductivity of the medium respectively. The magnetic field used to propel the ABF particles is about $2x10^{-3}$T as reported by [28], and the value of σ =0.05 according to [44]. The values of Ha for ϕ =0, and 0.8% are $1.4999x10^{-8}$, and 0.000749532 respectively. The values of Ha show that the effect of the magnetic field on the flow field is negligible, and thus on the Nusselt number. The energy needed to generate the magnetic field maybe needed to be added to pumping power, but due to the low value of the magnetic field, and the dilute nature of the suspensions we use, this extra energy is negligible. However, there are multiple ways to propel the particles such as thermal gradients, that can use the full energy stored in the system, but they are under development experimentally.

4.3 Solution Procedure

The governing equations have been discretized using the finite control volume method described in [45]. The SIMPLER algorithm was used, and the convective and diffusive terms are coupled using the power law scheme [45 ,46 and,47]. The pressure and the pressure correction equations have been derived from continuity. The discretized equations were solved using the tridiagonal matrix algorithm (TDMA). The equations of momentum and energy are considered converge if their residual reached a value of 10^{-6}or less. After careful consideration, a uniform 100 x 100 mesh was selected and implicit time integration was used with a time step equal to 0.1 s. The results of the in-house developed computer code were validated by comparison with available results in the literature, as shown in Figure10; the Nusselt number results show an excellent agreement with those of [37] for different Ra , for the case of single phase flow with working fluid as air.

4.4 Results and Discussion

In the following sections, the results obtained from the computer simulations are presented and discussed. The volume fractions selected range from 0.7% to 0.83% (which latter value is nearly at the limit of superfludity, where the viscosity of the fluid almost vanishes).

4.5 Temperature Contours and Streamlines

The transient development of the superimposed temperature contours and streamlines are shown in Figure 11 for the case of pure water (i.e. $\phi = 0.0$) and Ra =1.56 x 10^5 and Pr = 6.067($\left(\frac{c_p k}{\mu}\right)$. At the early stages of the heating process, at t = 10 s, Fig 11a, a thin thermal gradient started to form near the hot left wall. At the same time, the fluid flow is consisted of a large clockwise rotating pattern due to the rise of the fluid near the hot wall, simultaneously with the falling of the denser fluid near the cold wall. As time proceeds, at t = 100 s (Fig 11b), the thermal contours show more distortion and the portion of hotter liquid mixed with colder one due to the natural convection is increased. At t = 200 s and t = 300 s (Figs 11c and 11d), the thermal and flow field has reached a steady state. It is evident that the thermal contours are nearly straight lines, especially in the centre of the cavity, which is an apparent deviation from the pure conduction case, and a clear indication that natural convection is the dominant mechanism of heat transport.

Suspending a limited amount of self-propelled ABF carbon nanotubes into the water leads to a substantial decrease in the mixture viscosity. Specifically, suspending 0.8% by volume of self-propelled carbon nanotubes reduces the viscosity of the suspension according to Eq.17 by a factor of 25 times. This significantly increases the *Ra* from 1.56 x 10^5 to 3.77 x 10^6, and thus gives a boost for the buoyancy forces to overcome the viscous forces and increase the natural convection effects significantly, as is illustrated in Figure 12. From the very early stages of the simulation, the effects of natural convection start to appear as shown in Figure 12a (t = 10 s). Here, the temperature contours are distorted, especially in the middle of the cavity, not only near the hot walls as for the case of pure water (ϕ =0.0, Fig 11a), where conduction effects had a predominant role.

The velocity field is also distorted, with the centre of the flow pattern moving toward the upper left corner of the cavity. As the time proceeds to t = 100 s (Fig 12b), the temperature contours start to take the shape of horizontal lines due to natural convection effects, especially in the centre of the cavity. At the same time, the flow field consists of a large clockwise pattern that occupies the majority of the duct cross section, while in the middle and lower part of the cavity, small counter-clockwise cells start to appear, enriching the flow field and supplying an additional mechanism for fluid mixing, which is essential for any heat transfer fluids. At the later stages of the simulation, Figure 12 and Figure 12d, (t = 200 s and 300 s), the temperature contours nearly reach a steady state. The counter-clockwise rotating pattern grows in the middle of the duct, and its counterpart in the lower part of the duct disappears at the later stages of the simulation span, Figure 12d.

Figure 12 shows that suspending a very limited quantity of self-propelled particles can alter the flow field considerably, which favors the mixing process of the hot and cold portions of the solvent (i.e. water in the current case) and thus a better heat transfer rate can be achieved.

If we suspend non-active particles, the viscosity of the suspension increases due to the dissipation theorem. For this reason, we have chosen to compare the performance of the self-propelled nanofluid with a classical non-active nanofluid for the same volume fractions of particles. In our theoretical model, the only the difference between the self-propelled and the classical nanofluid is the way that the viscosity is predicted. For the case of a suspension of 0.8% by volume of non-active carbon nanotubes in water, the viscosity of the suspension will increase by a factor of 1.02, which shows that the viscosity of the suspension is nearly the same as that of pure solvent. This is also reflected in the value of *Ra* which is 1.48 x10^5, similar to that of pure water. Figure 13 shows the combined development of the flow field (streamlines) and the thermal field (temperature contours) for the non-active nanofluid. The development of both fields is like that of water, because the *Ra* for both cases is similar.

This very brief comparison shows the clear supremacy of self-propelled nanofluids over classical nanofluids and the pure water, at very small volume fraction of particles. This latter point is very encouraging, since it will help to maintain the stability of the suspensions over long operational periods.

To illustrate further the effect of adding self-propelled particles on the velocity field, the velocity magnitude was plotted along the mid plane (y = H/2) at t = 300s, and for the cases considered in the Figures 11 to13, as shown in Figure 14. Because we used the magnitude of the velocity in the x, and y direction, the values that appear in Figure 13 are always positive. For the case of pure water (ϕ = 0.0, Ra = 1.56 x 10^5), and the carbon nanotube and water nanofluid (ϕ = 0.8%, Ra = 1.48 x10^5), the flow consists of two local maxima, which is a result of the single flow pattern that occupies the square cavity. The maximum velocity is located near the walls, because the heavier fluid will decend near the cold wall, and at the opposite hot wall the lighter fluid will rise upwards. For the case of the self-propelled AFB carbon nanofluid (ϕ = 0.8%, Ra = 3.77 x 10^6), the velocity field consists of multiple local minima and maxima, as a result of the multi-cell nature of the flow, which dramatically enhances the heat transfer process through the convection mechanism. For simple comparison, the maximum velocity for the case of the self-propelled nanofluid is about 4 times larger, which a significant increase of its value, and thus the ability to mix and transfer heat.

We emphasize that the volume fraction of the particles used in both cases is extremely dilute. However, it has shown the effectiveness of self-propelled nanofluids compared with the classical nanofluids. Also, Eq.1 shows that for the case of self-propelled nanofluids, we can get a reduction of the viscosity with an increase of volume fraction, thus creating the right conditions for the formation of high conductive nanofluid.

4.6 Variation of Nusselt Number with Volume Fraction of Particles

Here we present the results for the average Nusselt number along the hot wall, this value being a key indicator of how much heat has been transferred to the fluid and the primary design parameter in developing any heat transfer equipment. As Eq. 20 indicates, Ra is a function of the thermal physical properties of the fluid used, the geometry and the operating conditions. The range of Ra utilized for different volume fractions is listed in Table 2. The values of the average Nusselt number at the steady state condition along the hot wall are presented in Table 3, for the cases of self-propelled and non-active nanofluids. As shown from the table, the self-propelled ABF carbon nanotube and water nanofluid is superior to its counterpart with non-active particles when tested under the same conditions. For example, for the case of ϕ = 0.83%, the Nusselt number of the self-propelled nanofluid is about 3 times higher than that of the non-active

nanofluid and also that of pure water. This great capacity to transfer heat is attributed to the increase in the value of the Rayleigh number as shown in Table 2, due the significant decrease in the viscosity of the fluid with the increasing volume fraction of the particles. The results of the Nusselt number test also confirm the scaling analysis conducted by Bejan [48] for natural convection flows inside closed ducts, in which the Nusselt number is a function of the Rayleigh number.

The main advantage of our newly proposed nanofluids is that they have very low viscosity, as shown in Table 4. Even when the volume fraction of the particles is extremely low, the viscosity of the suspension is 25 times less than the host water. This reduction in the viscosity has implications beyond the increase of the natural convection intensity; low viscosity means less pumping power for pumping the nanofluid, and thus increases the economic benefit. It should soon be possible design self-propelled nanofluids that have zero viscosity and flow without any direct pumping source. What we mean by the pumping source is a source that been used specifically for pumping the fluid such as a pump, the energy of the system will be employed mainly to alter the properties of the nanofluid. The concept of the self-propelled particles gives a variety of options for the type of energy that can be used to propel the particles. Very recent study show [33] that particles can move through the conversion of thermal energy into mechanical energy, and thus eliminate the need of an external field such as a magnetic field for the case of natural convection problems. However, those particles are under development there is no evidence yet that they can swim as pushers or been used.

We conducted a very recent scholarly search, and still, we did not find any rheological, or thermal transport properties measurements for the non-living colloidal active suspensions, the only experimental data available are those of the measurements of the relative viscosity of bacterial suspensions. However, this also shows the immaturity of active colloidal matter field and the broad avenues that are open for scientific inquiry. The theory that we presented in the current paper is valid for the living and non-living active matter, and thus our results are partially verified by experiments [20]. Very recently Slomka and Dunkel [49] showed by solving a unique form of Navier-Stokes equations for the active particles, and they predicted the viscosity of the suspensions, and also the structure of their flow field. They found that the

suspension viscosity is reduced, and the flow can be considered as inviscid flow (low viscosity flow), and the flow consists of many recalculating cells, similar to those predicted in the current paper. The significance of findings of [49] is that confirms the current existing experiments, and also current theory by using a new theoretical approach.

5 Conclusions

- A new type of a nanofluid is proposed by suspending ABF self-propelled metallic or carbon nanotube particles in water.
- According to theoretical and experimental work, the presence of self-propelled nanotube particles reduces the viscosity of the fluid compared with that of a classical, non-active nanofluid or a simple fluid such as water..
- Numerical simulations have been carried out to test the performance of the proposed ABF self-propelled nanofluid as a heat transfer fluid.
- For a low volume fraction of 0.8%, the Rayleigh number increased from $1.48x10^5$ for pure water or a classical nanofluid to $3.77x10^6$ for the ABF self-propelled nanofluid. This resulted in an increase in Nusselt number, reflecting heat transfer, by a factor of 3, a significant performance enhancement for heat transfer.
- The viscosity reduction would further contribute to a reduction in the energy requirement for pumping in heat transfer devices.

6 Directions for Future work

Our concept of self-propelled nanofluids can be used as a template to develop smart heat transfer fluids. For example, self-propelled nanofluids can change their viscosity by altering their swimming velocity and the concentration of their particles, and their thermal conductivity by the alignment of their particles and their concentration. Thus it might be possible to design particle systems to optimize their performance according to heating load. Also, it will be important if the particles can identify the hot spots and remove the heat efficiently from the surrounding area.

Acknowledgments

This research was conducted under the EU Framework 7 Marie Curie ITN Grant Number 607453: T-MAPPP: Training in Multiscale, MmultiPhase Particulate Processes, for which we express our gratitude.

References

1. Choi, S. U. S. "Enhancing thermal conductivity of fluids with nanoparticles." ASME-Publications-Fed 231 (1995): 99-106.
2. Maxwell, James Clerk. *A treatise on electricity and magnetism*. Vol. 1. Clarendon press, 1881.
3. Eastman, Jeffrey A., S. U. S. Choi, Sheng Li, W. Yu, and L. J. Thompson. "Anomalously increased effective thermal conductivities of ethylene glycol-based nanofluids containing copper nanoparticles." *Applied physics letters*78, no. 6 (2001): 718-720.
4. Choi, S. U. S., Z. G. Zhang, Wu Yu, F. E. Lockwood, and E. A. Grulke. "Anomalous thermal conductivity enhancement in nanotube suspensions." Applied physics letters 79, no. 14 (2001): 2252-2254.
5. Wang, Xiang-Qi, and Arun S. Mujumdar. "A review on nanofluids-part I: theoretical and numerical investigations." *Brazilian Journal of Chemical Engineering* 25, no. 4 (2008): 613-630.
6. Wang, Xiang-Qi, and Arun S. Mujumdar. "Heat transfer characteristics of nanofluids: a review." *International journal of thermal sciences* 46, no. 1 (2007): 1-19.
7. Angayarkanni, S. A., and John Philip. "Review on thermal properties of nanofluids: Recent developments." *Advances in colloid and interface science* 225 (2015): 146-176.
8. Keblinski, Phillbot, S. R. Phillpot, S. U. S. Choi, and J. A. Eastman. "Mechanisms of heat flow in suspensions of nano-sized particles (nanofluids)." *International journal of heat and mass transfer* 45, no. 4 (2002): 855-863.
9. Prasher, R., et al., " Measurements of nanofluid viscosity and its implications for thermal applications", *Applied Physics Letters*, 89, 2006, p.133108.

10. Sharma, Anuj Kumar, Arun Kumar Tiwari, and Amit Rai Dixit. "Rheological behaviour of nanofluids: A review." *Renewable and Sustainable Energy Reviews* 53 (2016): 779-791.
11. Tiwari, Arun Kumar, Pradyumna Ghosh, and Jahar Sarkar. "Heat transfer and pressure drop characteristics of CeO 2/water nanofluid in plate heat exchanger." *Applied Thermal Engineering* 57, no. 1 (2013): 24-32.
12. Murshed, S. M. S., K. C. Leong, and C. Yang. "Investigations of thermal conductivity and viscosity of nanofluids." *International Journal of Thermal Sciences* 47, no. 5 (2008): 560-568.
13. Einstein, Albert. "Eineneuebestimmung der moleküldimensionen." *Annalen der Physik* 324, no. 2 (1906): 289-306.
14. Jeffrey, Duncan James, and Andreas Acrivos. "The rheological properties of suspensions of rigid particles." *AIChE Journal* 22, no. 3 (1976): 417-432.
15. Mewis, Jan, and Norman J. Wagner. *Colloidal suspension rheology*. Cambridge University Press, 2012.
16. Nguyen, C. T., F. Desgranges, N. Galanis, G. Roy, Thierry Maré, S. Boucher, and H. AngueMintsa. "Viscosity data for Al 2 O 3–water nanofluid—hysteresis: is heat transfer enhancement using nanofluidsreliable?."*International Journal of Thermal Sciences* 47, no. 2 (2008): 103-111.
17. Saintillan, David, and Michael J. Shelley. "Theory of active suspensions." In *Complex Fluids in biological systems*, pp. 319-355. Springer New York, 2015.
18. Sokolov, Andrey, and Igor S. Aranson. "Reduction of viscosity in suspension of swimming bacteria." *Physical Review Letters* 103, no. 14 (2009): 148101.
19. Gachelin, Jérémie, GastónMiño, Hélène Berthet, Anke Lindner, Annie Rousselet, and Éric Clément. "Non-Newtonian viscosity of Escherichia coli suspensions." *Physical review letters* 110, no. 26 (2013): 268103.
20. López, HéctorMatías, JérémieGachelin, Carine Douarche, Harold Auradou, and Eric Clément. "Turning bacteria suspensions into superfluids." *Physical review letters* 115, no. 2 (2015): 028301.

21. Haines, Brian M., Andrey Sokolov, Igor S. Aranson, Leonid Berlyand, and Dmitry A. Karpeev. "Three-dimensional model for the effective viscosity of bacterial suspensions." *Physical Review E*, 80, no. 4 (2009): 041922.
22. Ryan, Shawn D., Brian M. Haines, Leonid Berlyand, FalkoZiebert, and Igor S. Aranson. "Viscosity of bacterial suspensions: Hydrodynamic interactions and self-induced noise." *Physical Review E* , 83, no. 5 (2011): 050904.
23. Alonso-Matilla, Roberto, Barath Ezhilan, and David Saintillan. "Microfluidic rheology of active particle suspensions: Kinetic theory." *Biomicrofluidics* 10, no. 4 (2016): 043505.
24. KATURI, J., et al. "Artificial micro-swimmers in simulated natural environments"., *Lab on a Chip*, 2016, vol. 16, no 7, p. 1101-1105.
25. LUO, Dan, et al. "Nanofluid of graphene-based amphiphilic Janus nanosheets for tertiary or enhanced oil recovery: High performance at low concentration". *Proceedings of the National Academy of Sciences*, 2016, p. 201608135.
26. Das, S.K., Choi, S.U., Yu, W. and Pradeep, T., 2007. Nanofluids: science and technology. John Wiley & Sons
27. Marshall, J.S. and Li, S., 2014. Adhesive particle flow. Cambridge University Press.
28. Zhang, Li, Jake J. Abbott, Lixin Dong, Kathrin E. Peyer, Bradley E. Kratochvil, Haixin Zhang, Christos Bergeles, and Bradley J. Nelson. "Characterizing the swimming properties of artificial bacterial flagella." *Nano letters* 9, no. 10 (2009): 3663-3667.
29. Ghosh, A., & Fischer, P. (2009). Controlled propulsion of artificial magnetic nanostructured propellers. *Nano letters*, *9*(6), 2243-2245.
30. Huang, Hen-Wei, et al. "Soft micromachines with programmable motility and morphology." *Nature Communications* 7 (2016).
31. Edd, Jon, Sébastien Payen, Boris Rubinsky, Marshall L. Stoller, and MetinSitti. "Biomimetic propulsion for a swimming surgical micro-robot." In*Intelligent Robots and Systems, 2003.(IROS 2003). Proceedings. 2003 IEEE/RSJ International Conference on*, vol. 3, pp. 2583-2588. IEEE, 2003.

32. Foroughi, Javad, Geoffrey M. Spinks, Gordon G. Wallace, Jiyoung Oh, Mikhail E. Kozlov, Shaoli Fang, TissaphernMirfakhrai et al. "Torsional carbon nanotube artificial muscles." *Science* 334, no. 6055 (2011): 494-497.
33. Li, Dongbo, Walter F. Paxton, Ray H. Baughman, Tony Jun Huang, J. Fraser Stoddart, and Paul S. Weiss. "Molecular, supramolecular, and macromolecular motors and artificial muscles." *MRS bulletin* 34, no. 09 (2009): 671-681.
34. Huang G, Mei Y. Helices in micro-world: Materials, properties, and applications. Journal of Materiomics. 2015 Dec 31;1(4):296-306.
35. Elgeti J, Gompper G. Self-propelled rods near surfaces. EPL (Europhysics Letters). 2009 Feb 6;85(3):38002.
36. Moradi M, Najafi A. Rheological properties of a dilute suspension of self-propelled particles. EPL (Europhysics Letters). 2015 Jan 23;109(2):24001.
37. Khanafer, Khalil, Kambiz Vafai, and Marilyn Lightstone. "Buoyancy-driven heat transfer enhancement in a two-dimensional enclosure utilizing nanofluids." *International Journal of Heat and Mass Transfer* 46, no. 19 (2003): 3639-3653.
38. Oztop, Hakan F., and Eiyad Abu-Nada. "Numerical study of natural convection in partially heated rectangular enclosures filled with nanofluids."*International Journal of Heat and Fluid Flow* 29, no. 5 (2008): 1326-1336.
39. Avramenko, A.A., Shevchuk, I.V., Abdallah, S., Blinov, D.G. and Tyrinov, A.I., 2017. Self-similar analysis of fluid flow, heat, and mass transfer at orthogonal nanofluid impingement onto a flat surface. Physics of Fluids, 29(5), p.052005.
40. Patteson, Alison E., Arvind Gopinath, and Paulo E. Arratia. "Active colloids in complex fluids." *Current Opinion in Colloid & Interface Science* 21 (2016): 86-96.
41. Hasadi, Yousef MF EL, and J. M. Khodadadi. "Numerical Simulation of Solidification of Colloids Inside a Differentially Heated Cavity." *Journal of Heat Transfer* 137, no. 7 (2015): 072301.
42. Rahman, M. M., Hakan F. Öztop, Michael Steele, A. G. Naim, Khaled Al-Salem, and Talaat A. Ibrahim. "Unsteady natural convection and statistical analysis in a

CNT–water filled cavity with non-isothermal heating."*International Communications in Heat and Mass Transfer* 64 (2015): 50-60.

43. Azizian, R., Doroodchi, E., McKrell, T., Buongiorno, J., Hu, L.W. and Moghtaderi, B., 2014. Effect of magnetic field on laminar convective heat transfer of magnetite nanofluids. International Journal of Heat and Mass Transfer, 68, pp.94-109.
44. Mahmoudi, A.H. and Abu-Nada, E., 2013. Combined effect of magnetic field and nanofluid variable properties on heat transfer enhancement in natural convection. Numerical Heat Transfer, Part A: Applications, 63(6), pp.452-472.
45. Patankar, Suhas. *Numerical heat transfer and fluid flow*. CRC press, 1980.
46. Hasadi, YM El, A. A. Busedra, and I. M. Rustum. "Laminar mixed convection in the entrance region of horizontal semicircular ducts with the flat wall at the top." *Journal of Heat Transfer* 129, no. 9 (2007): 1203-1211.
47. El Hasadi, Yousef MF. "Laminar Mixed Convection in the Entrance Region of Horizontal and Inclined Semicircular Ducts." *Advances in Mechanical Engineering* 5 (2013): 476537.
48. Bejan, Adrian. *Convection heat transfer*. John wiley& sons, 2013.
49. Słomka, J. and Dunkel, J., 2017. Geometry-dependent viscosity reduction in sheared active fluids. Physical Review Fluids, 2(4), p.043102.

	Water [38]	Carbon Nanotubes [39]
Density	997.1 kg/m^3	1350kg/m^3
Viscosity	8.9x10^{-4} Pa s	-
Specific Heat	4179 J/kg K	650 J/kg K
Thermal Conductivity	0.6 W/m K	1350 W/m K
Thermal Expansion Coefficient	2.1x10^{-4} K^{-1}	4.2x10^{-5} K^{-1}

Table 1. Thermophysical and transport properties for the solvent and the carbon nanotubes at 293K

Table 2. Corresponding Ra values for the case of self –propelled and non-active nanofluids

	Ra (non-active carbon nanotubes and water nanofluid)	Ra (self-propelled carbon nanotubes and water nanofluid)
ϕ = 0.7%	1.492x10^5	9.490x10^5
ϕ = 0.8%	1.481x10^5	3.793x10^6
ϕ = 0.83%	1.478x10^5	3.774x10^7

Table 3. Nusselt number values for different volume fractions of particles

	Nu (non-active carbon nanotubes and water nanofluid)	Nu (self-propelled carbon nanotubes and water nanofluid)
ϕ = 0.7%	5.342	8.915
ϕ = 0.8%	5.331	11.765
ϕ = 0.83%	5.328	17.972

Table 4. Variation of the viscosity of self-propelled nanofluids with particle concentration, and comparison with the viscosity of pure water

	Viscosity of suspension Eq. 17 (Pa.s)	Ratio between the viscosity of pure water and that of self-propelled nanofluid $\frac{\mu}{\mu_f}$
ϕ = 0.7%	0.0001424	6.25
ϕ = 0.8%	0.0000356	25
ϕ = 0.83%	3.56×10^{-6}	250

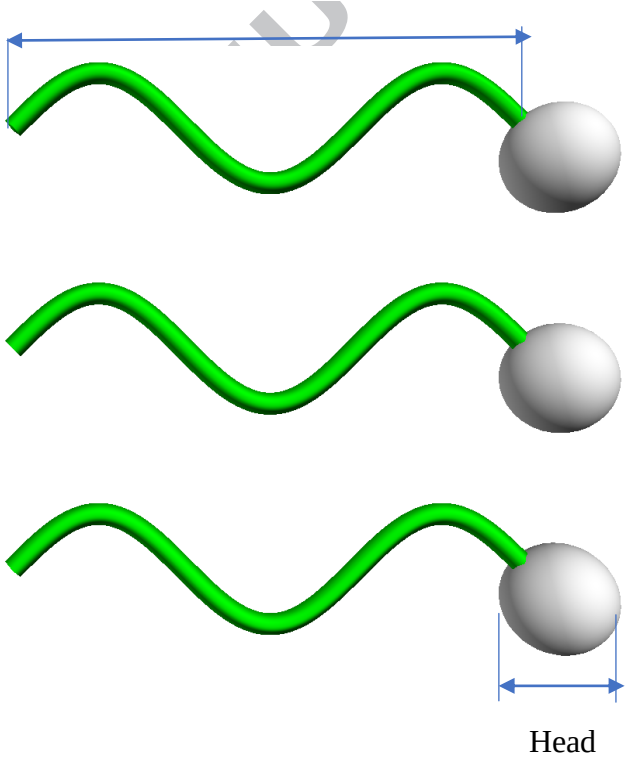

Figure 1. Proposed self-propelled particles

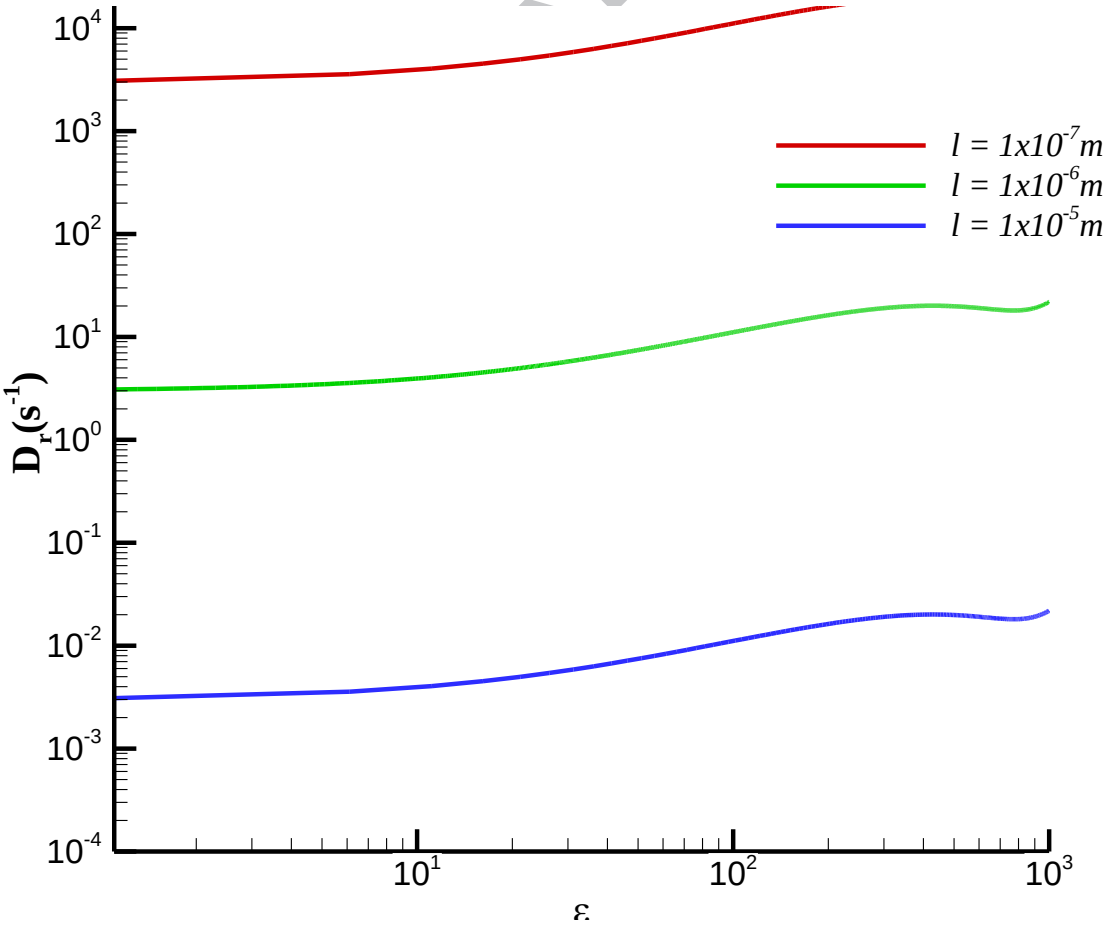

Figure 2. Variation of rotational diffusivity with aspect ratio of the particles and their length

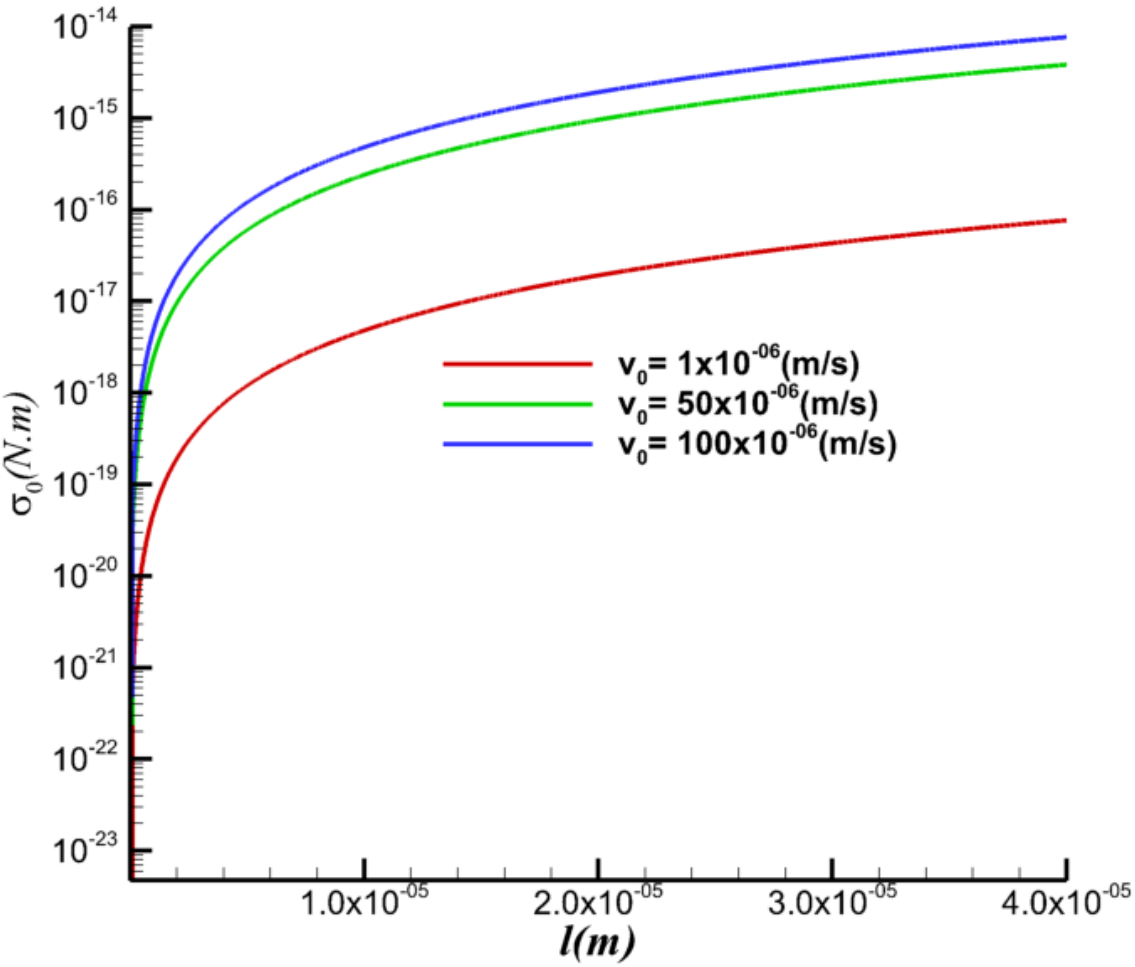

Figure 3. Variation of the activity of the particles (σ_0) with their length and swimming velocity

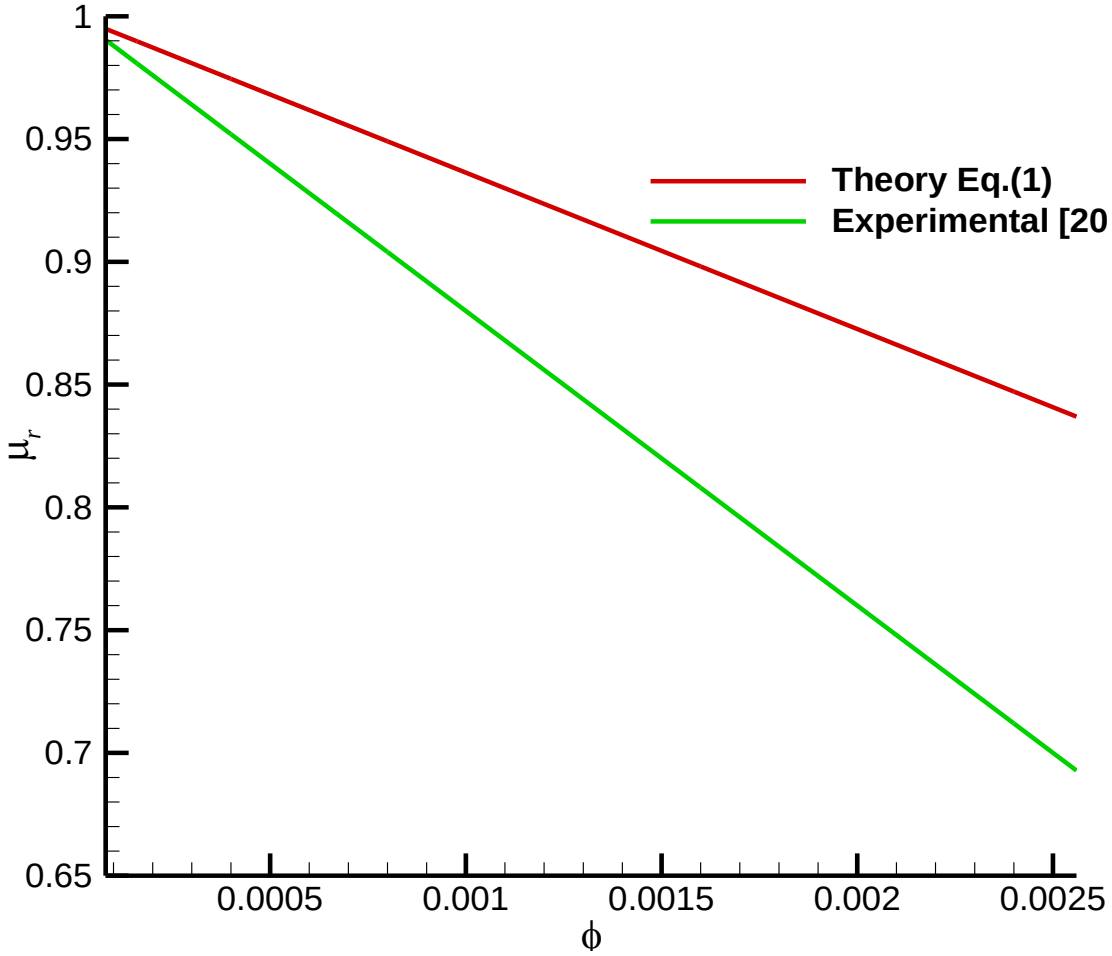

Figure 4. Comparison between experimental [20] and theoretical [Eq. 1] predictions of relative viscosity for suspensions of ABF particles swimming as pushers

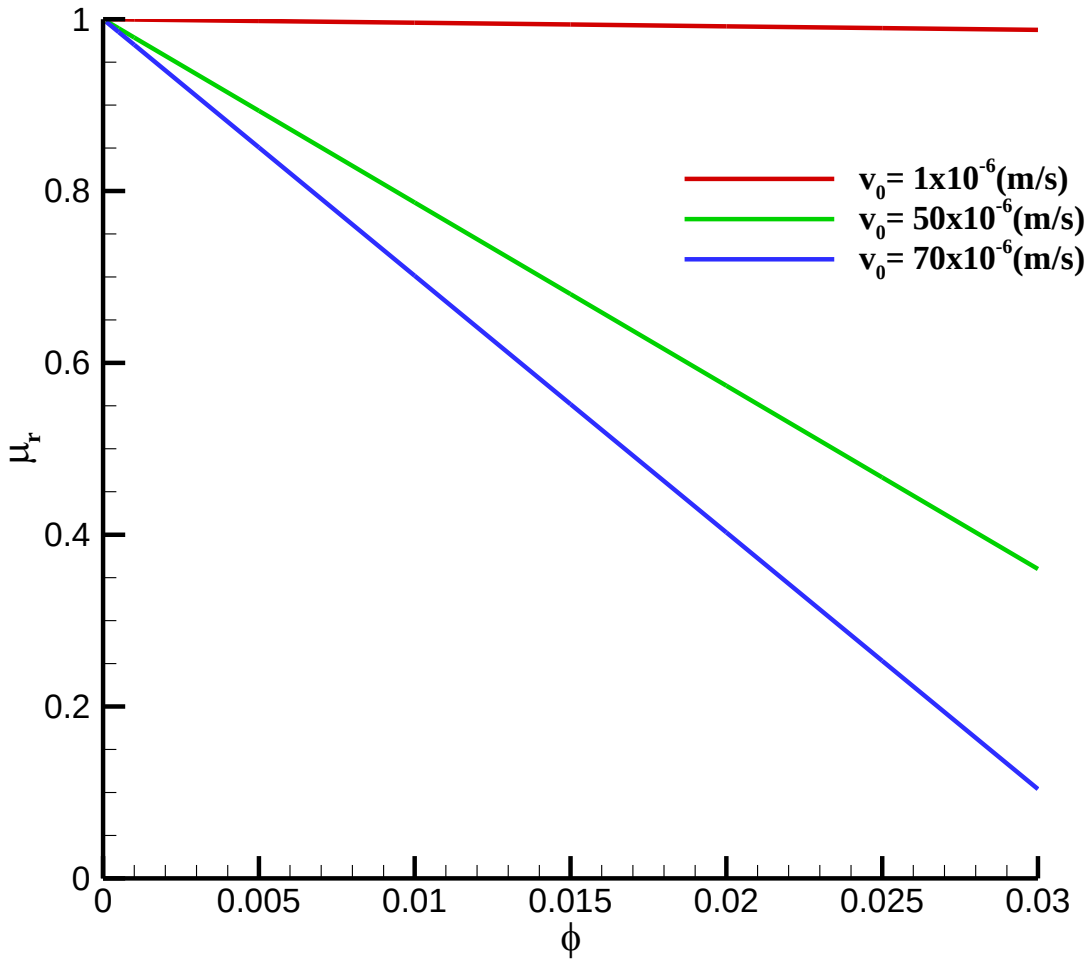

Figure 5. Variation the relative viscosity of the suspension μ_r with the volume fraction of the particles for the case of l = 1.0 x10^{-6} m and $\varepsilon = 10$, and for different swimming velocities

(a)

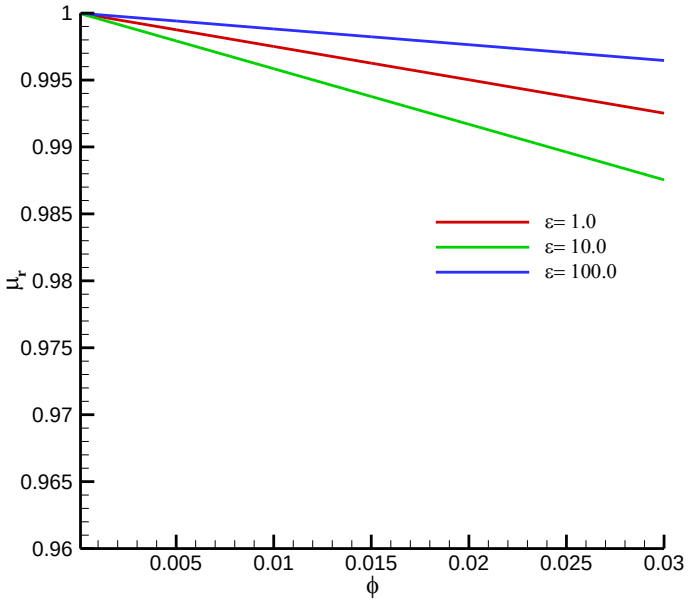

(b)

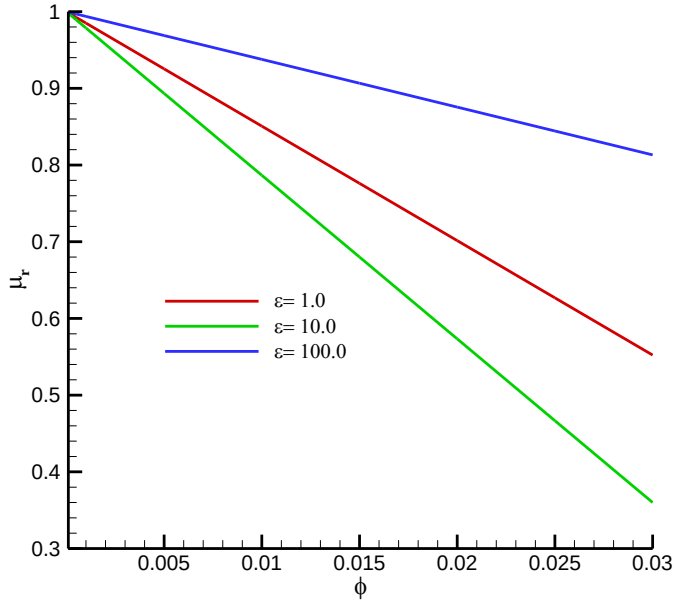

Figure 6. Variation of the relative viscosity of the suspension μ_r with the volume fraction of the particles for case of l = 1.0 x10^{-6} m and different aspect ratios ε(a) $\overline{v_0}$ = 1.0μms^{-1}; (b) $\overline{v_0}$ = 50.0μms^{-1}

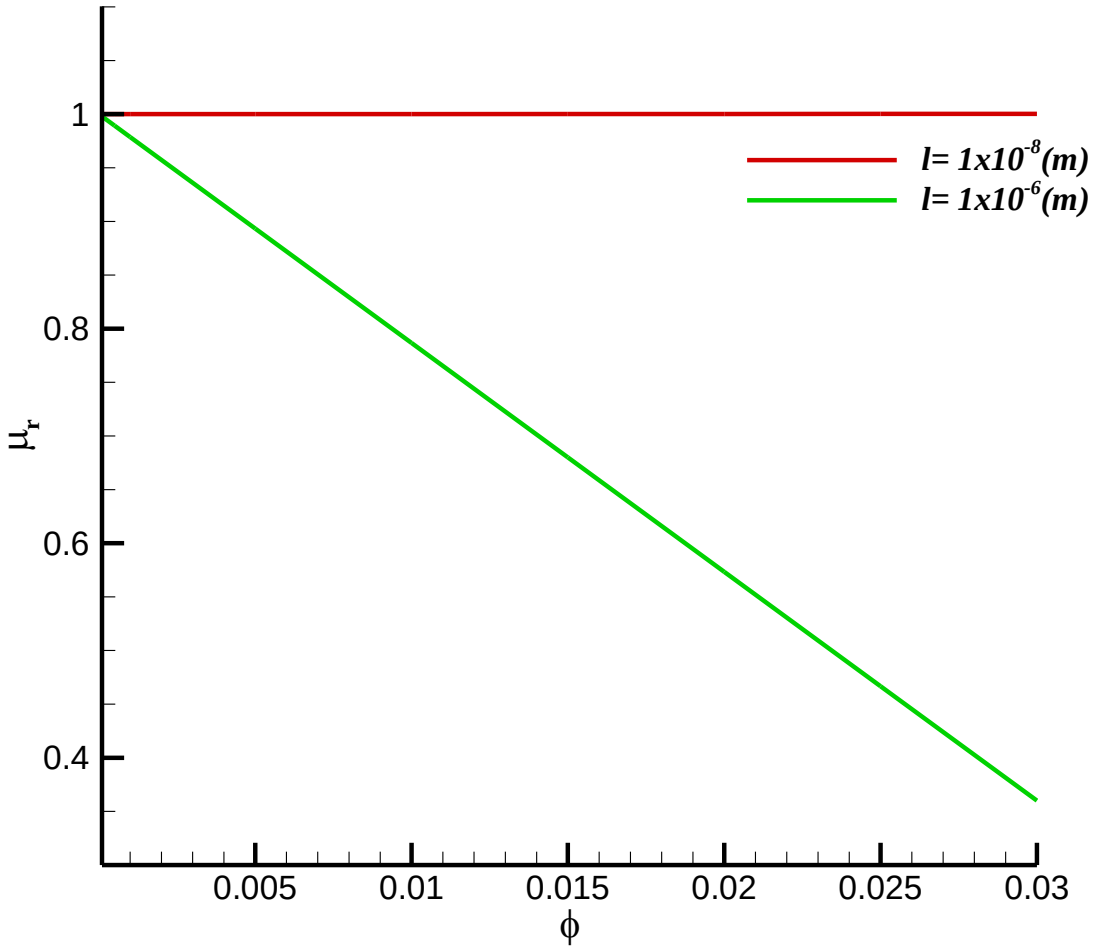

Figure 7. Variation of relative viscosity of the suspension μ_r with the volume fraction of the particles for case of $\varepsilon = 10$ and $\overline{v_0}$= 50.0 $\mu m s^{-1}$

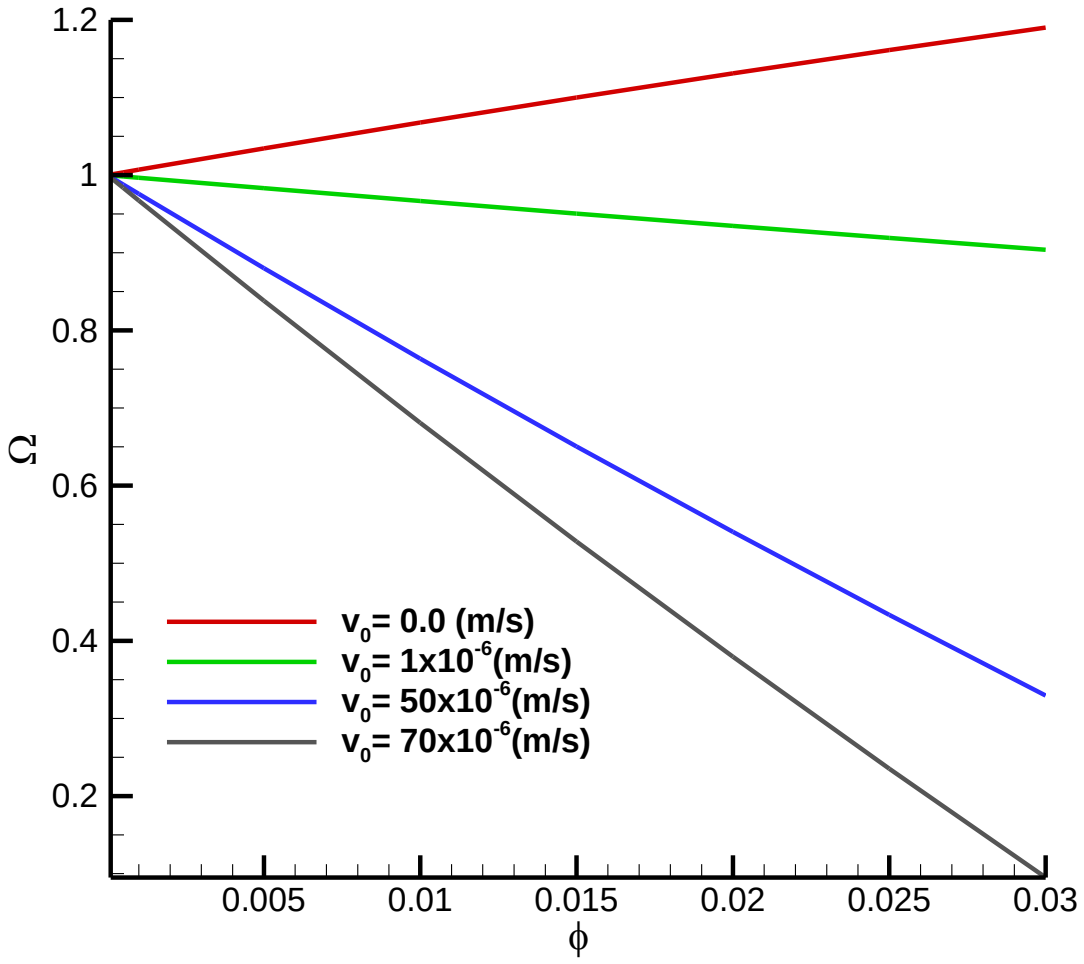

Figure 8. The variation of the efficiency parameter Ω with the volume of the particles for the case of l = 1.0 x10^{-6} m and $\varepsilon = 10$, and for different swimming velocities

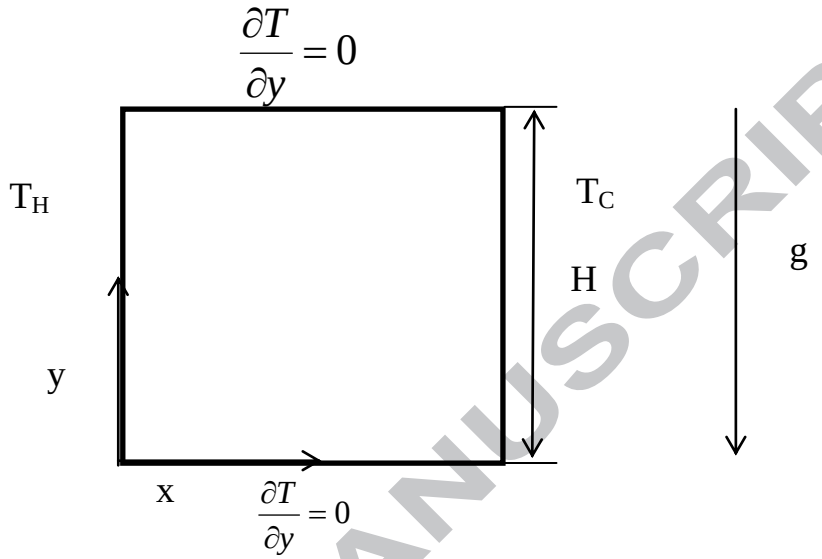

Figure 9. Geometry of the heat transfer model

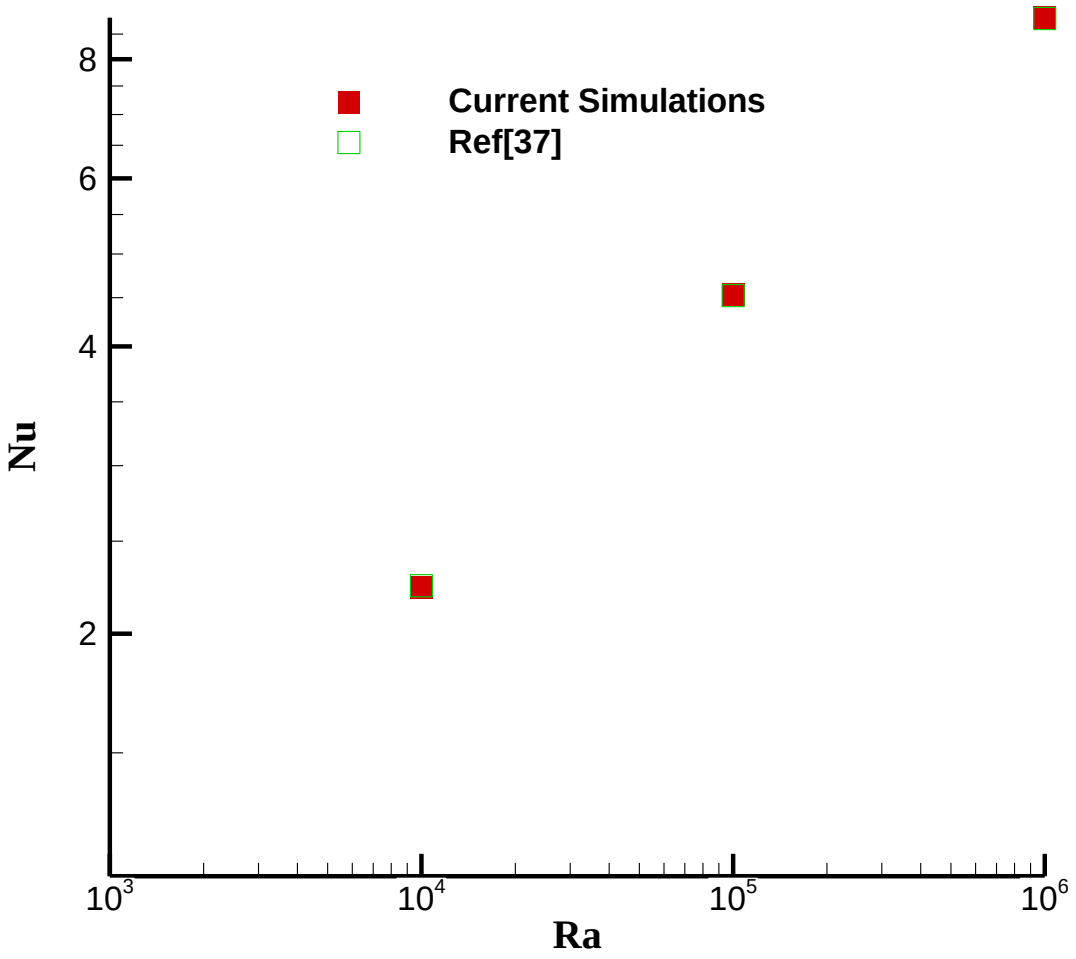

Figure 10 Comparison between the average Nusselt numbers obtained from the current simulations and the available data from the literature for different *Ra* numbers, *Pr* = 0.7

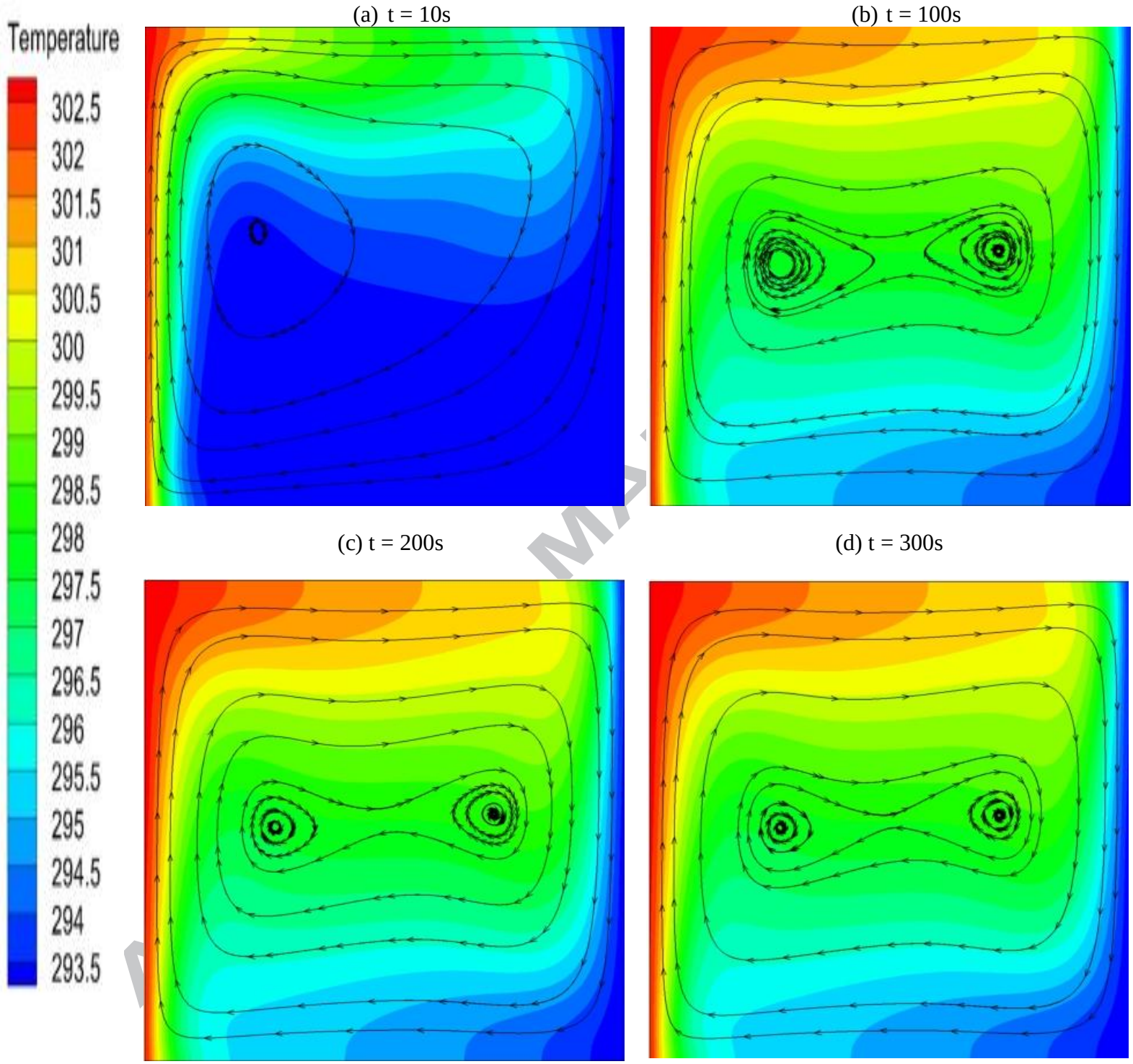

Figure 11. Transient development of the combined temperature contours and streamlines for the case of pure water; (ϕ = 0.0), Ra = 1.567x10^5

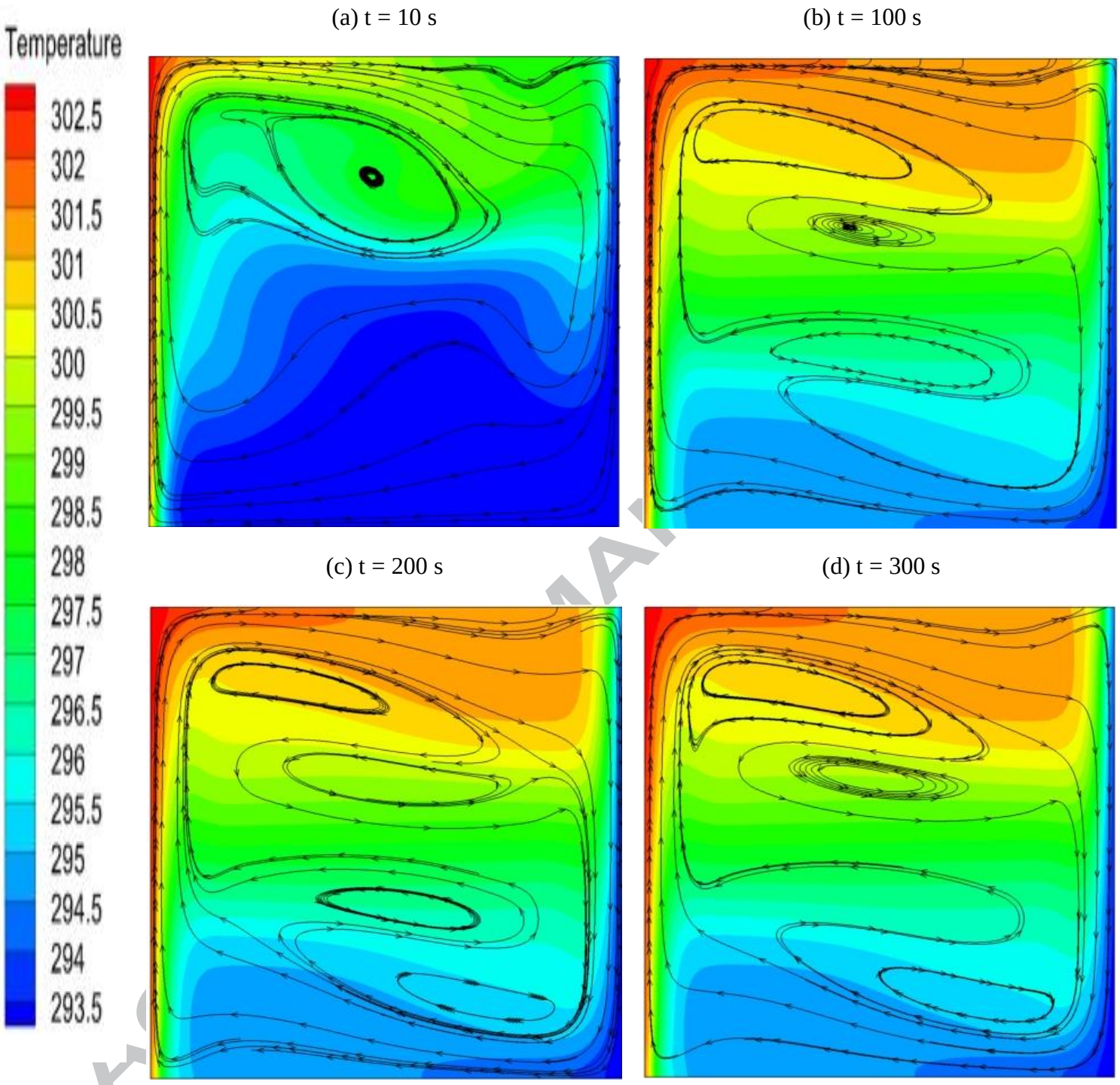

Figure 12. Transient development of the combined temperature contours and streamlines for the case of a self-propelled carbon nanotube nanofluid; (ϕ =0.8%), Ra = 3.793x10^6

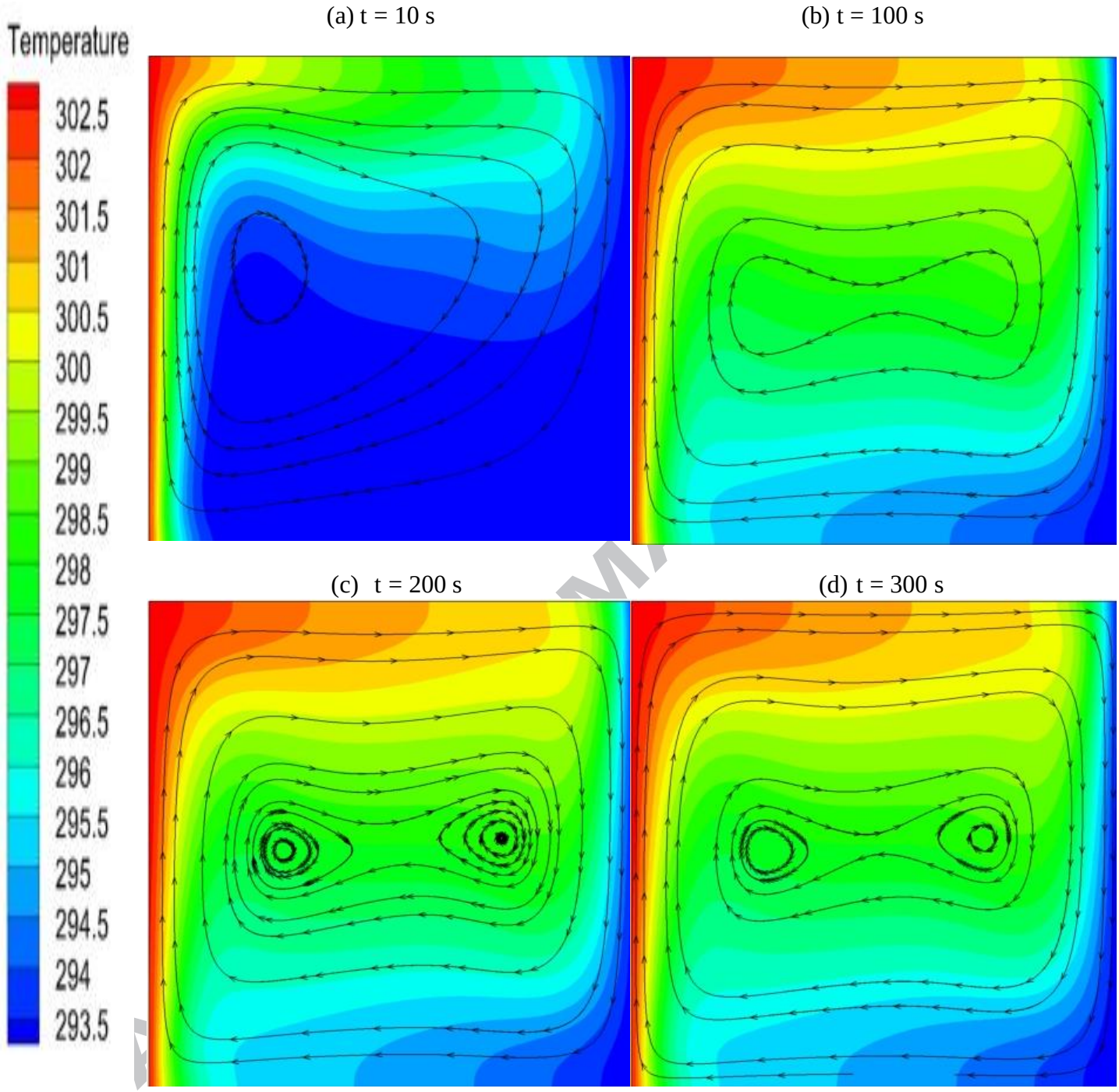

Figure 13 Transient development of the combined temperature contours and streamlines for the case of a non-active carbon nanotube nanofluid; (ϕ =0.8%), Ra = 1.481×10^5

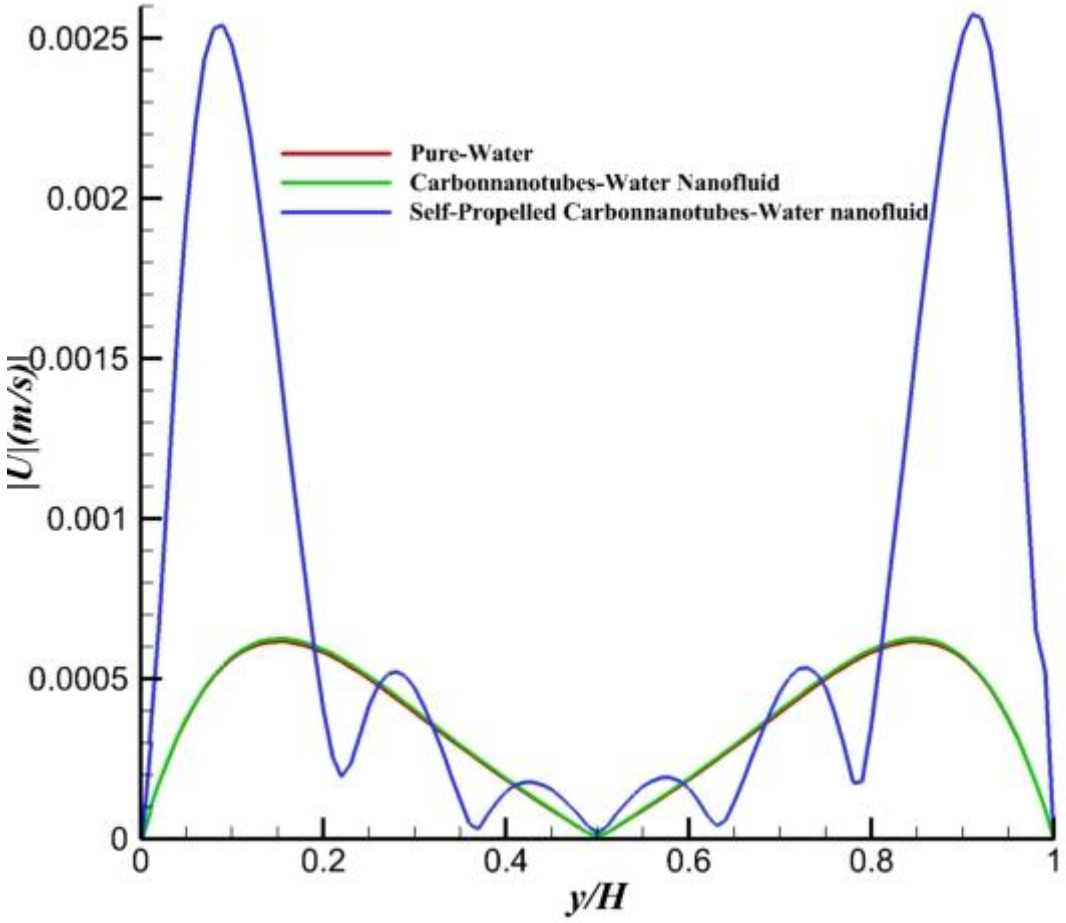

Figure 14 Variation of the magnitude of the velocity profile along x = 0.5 H at t = 300 s, for (a) Pure water (ϕ =0.0, Ra = 1.56 x 10^5); (b) non-active carbon nanotubes and water nanofluid (ϕ = 0.8%, Ra = 1.48 x10^5); (c) self-propelled carbon nanotubes and water nanofluid (ϕ = 0.8%, Ra = 3.77 x 10^6)

Highlights

- For the first time, Self-propelled nanofluids are introduced.
- The Self-propelled nanofluids exhibit positive thermo-physical properties.
- Their thermal conductivity increases with the volume fraction of particles.
- Their viscosity decreases with the volume fraction of particles.
- Their heat transfer rate is higher than pure water, and classical nanofluids.